Published in final edited form as:
Nanomedicine. 2014 April ; 10(3): 571–578. doi:10.1016/j.nano.2013.11.007.

Just-in-time vaccines: Biomineralized calcium phosphate core-immunogen shell nanoparticles induce long-lasting CD8+ T cell responses in mice

Weibin Zhou[†,a], **Albanus Moguche**[‡,a], **David Chiu**[†,§], **Kaja Murali-Krishna**[‡,b], and **François Baneyx**[†,§,*]

[†]Department of Chemical Engineering, University of Washington, Seattle, WA 98195

[‡]Department of Immunology, University of Washington, Seattle, WA 98195

[§]Department of Bioengineering, University of Washington, Seattle, WA 98195

Abstract

Distributed and on-demand vaccine production could be game-changing for infectious disease treatment in the developing world by providing new therapeutic opportunities and breaking the refrigeration “cold chain”. Here, we show that a fusion protein between a calcium phosphate binding domain and the model antigen ovalbumin can mineralize a biocompatible adjuvant in a single step. The resulting 50 nm calcium phosphate core-immunogen shell particles are comparable to soluble protein in inducing ovalbumin-specific antibody response and class switch recombination in mice. However, single dose vaccination with nanoparticles leads to higher expansion of ovalbumin-specific $CD8^+$ T cells upon challenge with an influenza virus bearing the ovalbumin-derived SIINFEKL peptide, and these cells produce high levels of IFN-γ. Furthermore, mice exhibit a robust antigen-specific $CD8^+$ T cell recall response when challenged with virus 8 months post-immunization. These results underscore the promise of immunogen-controlled adjuvant mineralization for just-in-time manufacturing of effective T cell vaccines.

Keywords

Nanovaccine; Nanocarrier; Biomineralization; Solid binding peptide

The next generation of vaccines should provide potent and long-lasting immune responses, have minimal side effects, and be safe, stable and easy to manufacture. This means moving from attenuated or killed pathogens towards purer, protein-based subunit vaccines. It also means compensating for the fact that subunit vaccines are less effective than traditional ones by including macromolecules or particles in the formulation to enhance, sustain and/or direct antigen immunogenicity.[1] These added compounds are known as adjuvants and function either as immunostimulants that are bound by pathogen-recognition receptors (e.g., Toll-like

[*]Corresponding author, baneyx@uw.edu (F. Baneyx).
[a]Contributed equally to this work
[b]Current address: Department of Pediatrics, Emory University School of Medicine, Atlanta, GA 30322

Conflict of Interest: The authors have no conflict of interest.

receptors) to boost immune responses, or as vehicles that optimize antigen delivery and presentation to the immune system.[1, 2]

Delivery vehicles are amenable to engineering design (which includes changes in structure, composition, morphology, physicochemical properties and conjugation of immunostimulatory or targeting molecules)[1, 3] and they hold potential for single dose, needle-free vaccination.[4] Aside from liposome-based and virus-like particles antigen delivery systems, several of which are already licensed or undergoing clinical studies, considerable attention has been paid to nanoparticles in the 20–100 nm size range because they freely enter the lymphatic system following subcutaneous or intramuscular injection.[5, 6, 2] Once these nanoparticles reach the lymph nodes, antigens coupled to their surface or entrapped within their cores have the opportunity to directly activate follicular B cells (which drive antibody-mediated responses), and to be efficiently taken up by dendritic cells which are powerful inducers of the T cell responses required for long-lasting humoral and cell-mediated immunity.[5, 7, 6, 8, 9] To date, such vaccinating nanoparticles have been made from polyesters (PLA/PLGA), polyanhydride (PVM/MA), and polysaccharides (inulin, alginate, hyaluronic acid and chitosan) which have a long record of biocompatibility (see ref.[2] and references within). However, while polymeric-based nanocarriers decorated with immunogens can induce robust antibody-mediated responses, achieving the robust $CD8^+$ T cell responses and memory that are critical to the development of therapeutic vaccines against viral infections and cancer[7, 8] can require considerable engineering (e.g., ref.[10]).

Another major challenge in vaccinology is that immunogens are often proteins which are prone to degradation, aggregation, oxidation or deamidation and that particulate vaccines are susceptible to colloidal instability.[9] This translates into limited shelf life and a need for stabilizing excipients and refrigeration. We believe that a solution to breaking the cold chain is distributed and just-in-time vaccine manufacturing. In this concept, a limited number of vaccine doses sufficient to treat the affected population are rapidly produced in rudimentary facilities at the time and place where they are most needed.

Solid binding peptides (SBPs) selected by combinatorial techniques for their ability to bind inorganic surfaces can be used to control materials nucleation, growth, crystallography, shape, size and function.[11–15] By engineering SBPs within larger protein frameworks, it is further possible to combine inorganic- and protein-associated activities, as we have for example demonstrated by using a fusion protein between a zinc sulfide binding peptide and an antibody-binding module to produce immunoglobulin-binding luminescent nanocrystals.[16, 17] The approach is appealing because an inorganic core-protein shell nanostructure of defined dimension can be produced in a single step and in aqueous solvents by the simple expedient of mixing protein with precursor salts.

Previously, we reported on the construction, expression and purification of TrxA::PA44, a derivative of *E. coli* thioredoxin A (TrxA) containing a 12 residues-long calcium phosphate (CaP) binding peptide called PA44 in place of the protein's native Cys-Gly-Pro-Cys active site loop. We used this fusion protein for the one-pot mineralization of sub-100 nm particles consisting of an amorphous calcium phosphate core stabilized by a capping protein shell. We further demonstrated that the resulting nanoparticles were slightly more effective than alum-adjuvanted TrxA::PA44 at eliciting a humoral response in C57BL/6 mice vaccinated subcutaneously as there was an about 3-fold increase in anti-TrxA IgG titers 21 days post-injection.[18] Here, we amplify on the just-in-time vaccine manufacturing concept by showing that a fusion protein between TrxA::PA44 and the model antigen ovalbumin (OVA) is suitable for the production of ≈ 50 nm CaP core-immunogen shell nanoparticles that support

antibody class switch recombination and are potent inducer of antigen-specific $CD8^+$ T cell responses and memory.

Materials and methods

DNA Manipulations

Plasmid pTrxA::PA44-OVA which encodes a fusion protein between a calcium binding variant of thioredoxin called TrxA::PA44[18] and chicken ovalbumin (OVA) was constructed as follows. A DNA cassette encoding OVA was PCR-amplified from plasmid pAc-neo-OVAl,[19] a kind gift from Mike Bevan (University of Washington), using primers 5′-CAACTCAGACCTAGGCATGGGCTCC-3’ and 5′-TCAGCTCTCTTCTTCTTAAGGGGAAACACAT-3′ to introduce *Avr*II and *Afl*II restriction sites. Plasmid pTrxA::PA44,[18] and primers 5’-GCGTCGACCTTAAGTAATCGTACAGGGTAGT-3’ and 5’-GCAAGCCTAGGTTAGCGTCGAGGAAC-3’ were used to introduce the same restriction sites in a large DNA fragment specifying most of pTrxA::PA44. Amplified DNAs were digested with *Avr*II and *Afl*II and the cassette encoding OVA was ligated to the pTrxA::PA44 backbone that had been dephosphorylated with shrimp alkaline phosphatase. Construct integrity was verified by DNA sequencing. A plasmid encoding an OVA-TrxA::PA44 fusion protein was also built but no protein expression was detected (presumably due to the fact that a stem-loop structure at the 5’ end of the ovalbumin mRNA interferes with transcription)[20] and the construct was abandoned.

Protein expression, refolding and purification

BL21(DE3) cells harboring pTrxA::PA44-OVA were grown to $A_{600} \approx 0.5$ at 37°C in 500 mL of LB medium supplemented with 34 μg/mL chloramphenicol. Flasks (2L) were transferred to a water bath held at 25°C for 10 min and protein synthesis was induced by addition of 1 mM of isopropyl β-D-thiogalactopyranoside (IPTG). After 4h, cells were harvested by centrifugation at 3,000 *g* for 15 min, and resuspended in 20 mM Tris-HCl, pH 7.5 supplemented with 2.5 mM EDTA and 1 mM PMSF to an A_{600} of 50. Cells were disrupted by three cycles of homogenization on a French pressure cell operated at 10,000 psi and the lysate was separated into soluble and insoluble fractions by centrifugation at 14,000 *g* for 15 min.

Pellets containing the inclusion body material were resuspended by vortexing into 5 mL of buffer A (20 mM Tris-HCl, pH 7.5, 2.5 mM EDTA, 1 mM PMSF) supplemented with 1% (v/v) Triton X-100. Following centrifugation at 14,000 *g* for 10 min, the supernatant was discarded and the wash step was repeated once as above and twice more using buffer A alone. Washed inclusion bodies were resuspended in 15 mL of buffer A supplemented with 6 M of guanidium hydrochloride and incubated at room temperature for 1h with gentle shaking. After removing any remaining insoluble material by centrifugation at 14,000 *g* for 10 min, unfolded protein aliquots (5 mL) were refolded by dropwise addition into 95 mL of buffer A with gentle stirring. The remaining guanidium hydrochloride was removed by 16 h dialysis against 2L of buffer A, with buffer changes at 1h and 4h. The refolded protein was filtered through a 0.45 μm cartridge and loaded on a 1 cm column packed with 5 g of DE52 Cellulose (Whatman) pre-equilibrated in buffer A. The column was developed at 1 mL/min in buffer A and TrxA::PA44-OVA was eluted with 200 mM NaCl after a 50 mM NaCl step to remove contaminants. Protein concentrations were determined using the Thermo Bradford assay with BSA as a standard, and lack of endotoxin contamination was confirmed using the Pyrogent-5000 LAL assay kit (Lonza).

Nanoparticle mineralization and characterization

Calcium phosphate (CaP) nanoparticles were produced essentially as described.[18] Briefly, 200 μL of a 16.7 mM $Ca(NO_3)_2$ solution were added dropwise to 1.8 mL of a well-stirred mixture of 1.11 mM $(NH_4)_2HPO_4/NH_4H_2PO_4$, pH 7.5 supplemented with 4.44 μM TrxA::PA44-OVA that had been previously incubated at 4°C for 30 min. After addition of the calcium, the mixture was allowed to age at 4°C for 2 h with high-speed stirring with a small magnetic bar. Endotoxin-free water and disposable glassware cleaned with acetic acid, acetone and water was used in all steps.

Hydrodynamic diameters were measured by dynamic light scattering (DLS) on a Nano-ZS Zetasizer (Malvern). For SEM imaging, samples (≈ 100 μL) were allowed to contact a clean, ≈ 1 cm^2 silicon wafers for 30 min and excess fluid was removed by wicking with a laboratory tissue. The substrate was rinsed with ddH_2O to remove salts, air dried and coated with a 7–10 nm Au/Pd film. Micrographs were taken with a FEI Sirion SEM at 10 keV acceleration voltage.

Mice, immunization and challenge

All mice were used in accordance with the guidelines of the Institutional Animal Care and Use Committees of the University of Washington. A total of 24 C57BL/6J mice were purchased from Jackson Laboratory. One group (n=8) was immunized with 18 μg of TrxA::PA44-OVA in 1 mM ammonium phosphate. A second group (n=8) was immunized with 18 μg of TrxA::PA44-OVA@CaP in 1.67 mM calcium nitrate and 1 mM ammonium phosphate. The final group (n=8) was left unimmunized to serve as a control. A total volume of 200 μl of control protein or nanoparticles (≈ 0.005% v/v) was administered by sub-cutaneous injection. Mice were challenged at 4 months (n=1 animal per cohort) or 8 months (n=6 animals per cohort) post-immunization with 1000 plaque forming units (PFU) of a recombinant influenza virus A/WSN/1933 (WSN) carrying the transgene for chicken ovalbumin (WSN-OVA).[21] Following viral challenge, spleens were extracted from half of the animals on day 7 while the remaining mice were monitored for weight loss every other day. Animals were sacrificed if they lost more than 20% of their starting body weight.

Antibody titration

At 1, 2 and 4 weeks post-vaccination, mice were bled and serum was analyzed for ovalbumin specific antibodies. In brief, 96-well micro-plates (Corning #3369) were coated overnight at 4°C with chicken ovalbumin (Fisher Scientific #BP2535-5) in 0.2M anhydrous sodium carbonate, 0.2M sodium bicarbonate, pH 9.2. Non-specific binding was blocked using 5% fat free milk in 0.05% Tween Tris-buffered saline at 4°C overnight. After discarding the blocking buffer, twofold serial dilutions of serum samples (or for standards curve, titrated anti-chicken ovalbumin monoclonal antibody; Gene Script #A00852) were added to the plates. After 2h incubation at 37°C, the plates were washed 3 times with 0.5% fat free milk in 0.05% Tween Tris-buffered saline. Anti-mouse IgG or anti-mouse IgM conjugated to Horseradish Peroxidase (Millipore) were added and plates were incubated at 37°C for 1h. After 3 wash cycles, plates were developed with TBM reagent (Fisher Scientific) for 20 min. Reactions were stopped by addition of 2 M sulfuric acid and absorbance was read at 450 nm using a plate reader (Molecular Devices).

Flow cytometry analysis

Spleen, lung, blood or pulmonary training lymph nodes single cell suspensions were prepared essentially as reported.[22] In brief, single cell suspensions of intra-parenchymal lung lymphocytes were prepared by Liberase-Blendzyme (Roche) digestion of perfused lungs in the presence of DNAse (Sigma-Aldrich). Single cell lymphocyte cell suspensions

were also made from spleen and lung draining lymph node by crushing the tissues between two frosted glass slides. Red blood cells in the above single cell suspensions were lysed using the ACK RBC lysis buffer (Invitrogen). The cells were subsequently stained for surface markers using anti-mouse monoclonal antibodies against CD3 (clone 145-2C11), CD4 (clone RM4-5), CD8 (clone 53-6.7), CD44 (clone IM7) and CD62L (clone MEL-14) obtained from Biolegend. Ova-specific $CD8^+$ T cells were detected using the major histocompatibility complex class I ($H2K^b$) restricted SIINFEKL tetramer (OVA 257–264) tetramerized to APC or PE-conjugated streptavidin. The antibodies and tetramer were diluted in a buffer containing 0.1% sodium azide and 2.5% fetal bovine serum and Fc receptor blocking antibodies (anti-mouse CD16/32). All stains were done at saturating concentrations and 4°C for 30 min. To detect IFN-γ, aliquots of single cell lymphocytes suspensions were stimulated with SIINFEKL peptide and incubated for 4 h in complete RPMI (RPMI 1640 supplemented with 10% FCS, 2 mM L-glutamine, 10 mM Hepes, 0.5 μM 2-mercaptoehtanol, 100 U/ml penicillin, and 100 μg/ml streptomycin) in the presence of monensin (BD Golgi-Stop). Cells were then stained for surface markers as above and, after permeabilization, stained for IFN-γ (XMG1.2, BD) and incubated at 4°C for 30 min. Cells were fixed in 1% paraformaldehyde solution in PBS and analyzed on a LSRII flow cytometer (BD) and the FlowJo software (Tree Star).

Results

Construction and purification of a calcium phosphate-binding ovalbumin variant

To further explore the potential of CaP core-protein shell nanoparticles for vaccine formulation, we fused TrxA::PA44 to ovalbumin (OVA), thus combining a domain capable of producing CaP nanoparticles by surface capping[18] with a model antigen (Fig. 1A). Because the resulting fusion protein accumulated as inclusion bodies when overexpressed in *E. coli* (Fig. 1B), we purified TrxA::PA44-OVA by unfolding it in guanidium hydrochloride, refolding it by dilution, and removing trace contaminants and endotoxins by ion exchange chromatography as detailed in Materials and Methods.

Protein-aided fabrication of calcium phosphate core immunogen shell nanoparticles

We first sought to determine how the presence of the 45-kDa OVA extension would affect the ability of TrxA::PA44 to control the mineralization of CaP nanoparticles. To this end, 4 μM of fusion protein in calcium nitrate buffer was added dropwise and with high agitation to a sodium phosphate solution essentially as described[18] and the mixture was allowed to age for 2h. SEM imaging of gold-palladium coated samples (Fig. 2A) revealed the presence of well-dispersed spheroids that were 75 ± 12 nm in diameter based on manual measurement of n = 50 particles. This size is in good agreement with a hydrodynamic diameter of 44 ± 3 nm obtained by dynamic light scattering (DLS) once the 7–10 nm thickness of the Au/Pd coating used for SEM visualization is taken into account. It is also comparable to the size of particles that we previously obtained with unfused TrxA::PA44 (70 ± 15 nm by SEM and 60 ± 20 nm by DLS).[18] Inspection of higher resolution SEM images (Fig. 2B) suggests that each nanoparticle is formed by the agglomeration of nanometer size CaP clusters whose accretion is quenched upon adsorption of the fusion protein. We conclude that the presence of a full-length OVA domain does not interfere with the ability of TrxA::PA44 to prevent bulk CaP precipitation and to stabilize colloidal suspensions of ≈ 50 nm particles by surface capping.[18]

Biomineralized nanoparticle induce antibody class-switch recombination

Class switch recombination (CSR) occurs in B cells after they have been exposed to antigen and costimulatory signals, proliferated, differentiated and migrated to the germinal centers of secondary lymphoid organs (spleen, lymph nodes and tonsils).[23, 24] CSR is typically

dependent upon $CD4^+$ T helper cells[25, 26] and involves deletional recombination events that target the heavy chain constant region of immunoglobulins and redirect antibody production from IgM and IgD classes to the IgG, IgA and IgE isotypes. To determine if TrxA::PA44-OVA-mineralized nanoparticles (thereafter referred to as TrxA::PA44-OVA@CaP) would induce CSR, C57BL/6 mice were injected subcutaneously with the nanomaterial (Figure 3, closed symbols) or the same amount of purified TrxA::PA44-OVA (open symbols) and serum ovalbumin-specific antibodies were quantified. Figure 3A shows that both formulations induced comparable levels of ovalbumin-specific pentameric IgM, the first antibody produced, with a production peak at 7 days post-immunization followed by a rapid decline in serum levels. As expected for a typical CSR process, the concentration of OVA-specific IgG and IgG1 subclass antibodies started to rise at day 7 in both populations, reached a plateau at day14 and remained elevated after 4 weeks (Figures 3B–C). Clearly, the TrxA::PA44-OVA@CaP formulation does not interfere with CSR which implies that the particles are capable of inducing antigen-specific $CD4^+$ T cell responses. Nonetheless, the lack of difference in the levels or dynamics of IgM, IgG and IgG1 accumulation indicates that there is no distinct advantage in using the nanoparticle formulation over free protein if one seeks to induce humoral immunity. Why we did not observe a small increase in antigen-specific IgG titers as we previously did when using TrxA::PA44-mineralized particles remains unclear but may be related to differences in immunization protocol, more efficient uptake of the larger TrxA::PA44-OVA by dendritic cells, or to the higher immunogenicity of the OVA domain relative to TrxA.

Biomineralized nanoparticle are more efficient than free protein at inducing antigen-specific $CD8^+$ T cell responses

Protein immunogens that have been uptaken by antigen presenting cells (e.g., dendritic cells) are processed into peptides in the endolysosome, loaded onto major histocompatibility complex (MHC) class II molecules, and exported to the cell surface for stimulation of $CD4^+$ T helper cells. The latter collaborate with activated B cells to generate antibody-producing plasma cells and memory B cells. In a process known as cross-presentation, antigens may also be loaded onto MHC class I molecules to prime $CD8^+$ T cells which produce immune cytokines such as interferon (IFN)-γ and tumor necrosis factor (TNF)-α, play prominent roles in clearing viral infections and eradicating tumors.[8]

Most of the currently licensed vaccines confer protection through the induction of antigen specific antibody responses.[7] However, some infections are not easily controlled by antibodies and require the induction of antigen specific $CD4^+$ T cells and cytotoxic $CD8^+$ T cells for protection. Because soluble and nanoparticle-bound TrxA::PA44-OVA induce similar antibody responses and support CSR (Figure 3), both formulations likely activate similar $CD4^+$ T cell responses. To determine if antigen-specific $CD8^+$ T cells responses would be different, we performed a preliminary challenge experiment at 4 months in which one mouse from the groups immunized with TrxA::PA44-OVA, TrxA::PA44-OVA@CaP or left unimmunized, was subjected to intranasal administration of WSN-OVA. This recombinant influenza virus contains the ovalbumin-derived (OVA 257–264) SIINFEKL peptide in the stalk of the neuraminidase capsid protein.[21] Mice were sacrificed 12 days after viral infection and their lungs were analyzed for antigen specific $CD8^+$ T cell responses against OVA by flow cytometry. Figure 4A shows that the mouse vaccinated with TrxA::PA44-OVA@CaP induced a 2.5 fold higher expansion of antigen (SIINFEKL)-specific $CD8^+$ T cell relative to the animal immunized with free protein, and a 40-fold higher expansion compared to the unimmunized animal. Furthermore, when these cells were re-stimulated *in vitro* with the SIINFEKL peptide, they produced twice as much IFN-γ than those from the animal vaccinated with free protein (Figure 4B). On the other hand, while lung cells from both immunized animals produced significantly more TNF-α upon peptide

stimulation relative to cells from naïve mice, the vaccine formulation had no influence on the levels of this cytokine (Figure 4C). Although conducted on a single mouse per group, these experiments revealed an encouraging trend: immunization with the nanoparticle formulation leads to larger numbers of antigen specific $CD8^+$ T cells at the infection site and these cells are capable of producing high-levels of the antiviral cytokine IFN-γ.

Nanoparticle-induced $CD8^+$ T cells are long-lived and undergo enhanced recall responses

A critical concern for vaccine development is the longevity of antigen-specific responses which often wane after 6 months.[27] To determine how long nanoparticle-induced $CD8^+$ T cell memory would last, we waited an additional four months to repeat the intranasal WSN-OVA challenge. In this 8 months study, we measured OVA-specific $CD8^+$ T cells in the spleen 7 days post-infection and monitored mice for weight loss. We used three animals per group for each of these two experiments. Figure 5A shows that antigen-specific T cells could be detected in the spleen of mice from each of the three groups. However, expansion was highest in mice immunized with TrxA::PA44-OVA@CaP. Further underscoring the performance of nanoparticles in eliciting T-cell memory, there were 4-times more SIINFEKL tetramer-binding cells in the spleen of animals immunized with TrxA::PA44-OVA@CaP compared to those vaccinated with free protein (Fig. 5B). These results are comparable to, and in complete agreement with, the preliminary data of Fig. 4 in which mice were challenged at 4 months post immunization. Finally, although infected animals immunized with TrxA::PA44-OVA@CaP lost weight at an initial rate that was comparable to that of control mice, we observed a small but statistically significant difference in weights at day 8 (Fig. 5C). Moreover, whereas two animals from the unimmunized group and two animals from the TrxA::PA44-OVA-vaccinated group were sacrificed at day 9 because they had lost over 20% of their original weight, all mice from the TrxA::PA44-OVA@CaP-immunized group retained 85 to 90% of their original weight at day 10.

Discussion

In this study, we have shown that *ca.* 50 nm calcium phosphate core-immunogen shell nanoparticles fabricated in a single-pot reaction using a fusion protein between a CaP-binding moiety and OVA are effective elicitors of cell mediated immunity. More specifically, we found that immunization with this formulation is vastly superior to the use of free protein in eliciting long-lasting $CD8^+$ T cell responses with high-level IFN-γ production and enhanced recall responses. This may be due to the fact that the mean hydrodynamic diameter of our nanoparticles falls within the 40–50 nm size that has been determined to be optimal for delivery to dendritic cells in the lymph nodes[28, 29, 10, 30] and for antigen cross-presentation in mice[31]. In addition, the presence of multiple immunogens on each nanoparticle is likely to improve loading on class I MHC molecules as cross-presentation of antigens attached or adsorbed to particles in the 20 nm to 3 μm size range is more efficient than with soluble proteins.[32, 33] The role of the inorganic core is less clear. A possible explanation is that the kinetics of dissolution of amorphous CaP nanoparticles[34] and the associated rate of antigen release in the acidic phagosomes where 50 nm diameter particles are preferentially transported[35] are optimal for antigen cross-presentation.[36]

He and coworkers have previously entrapped/adsorbed viral proteins within micrometer-sized CaP aggregates by co-precipitation and reported that this formulation induces a robust antibody response in mice.[37, 38] By analogy to aluminum-based adjuvants,[39] this is likely due to the ability of the CaP aggregates to function as immunogen depots that enhance T helper cell responses through long-lasting antigen release. The small nanoparticles that we produce through our biofabrication scheme are morphologically very different. They are expected to readily drain to the lymph nodes[5] and are thus unlikely to function as antigen

depots. In addition, while multiple epitopes decorate each nanoparticle, they are not presented in the repetitive geometry that is necessary for efficient cross-linking of B cell receptors and strong B cell activation.[6, 40] It is therefore not surprising that the antibody response observed with the TrxA::PA44-Ova@CaP is comparable to that obtained with the soluble protein. Nevertheless, our nanoparticle formulation activates $CD4^+$ T helper cell responses since it supports CSR.[25, 26] If a strong antibody-mediated response is desired, it should be straightforward to modify the design by tethering or adsorbing Toll-like receptor (TLR) ligands such as CpG-containing oligodeoxynucleotides since these molecules have proven quite effective at enhancing humoral immunity.[41, 42]

Conclusions

Just-in-time vaccine manufacturing requires simple production schemes with rudimentary equipment and an end-product efficacy comparable to, or superior to that of conventionally manufactured vaccines. Here, we have shown that a model immunogen consisting of a fusion protein between a calcium phosphate-binding segment and OVA can be used to mineralize its own adjuvant in a single mixing step. In mice, the resulting 50 nm CaP core-immunogen shell nanoparticles induce an OVA-specific antibody response and CSR comparable to the free protein. However, they are much more powerful at inducing OVA-specific $CD8^+$ T cell populations that secrete high levels of IFN-γ, are long-lived and exhibit enhanced recall responses. The strategy described here should prove useful for the distributed and on-demand production of T cell mediated therapeutic vaccines that hold great promise for the treatment of infectious diseases but have so far been very challenging to produce.

Acknowledgments

We are grateful to Sathana Kitayaporn for help with SEM imaging. Part of this work was conducted at the University of Washington Nanotech User Facility, a member of the NSF National Nanotechnology Infrastructure Network.

This work was supported by a Grand Challenge Exploration grant from the Bill and Melinda Gates Foundation and by NIH awards U19ES019545 and R01AI086133.

References

1. Reed SG, Bertholet S, Coler RN, Friede M. New horizons in adjuvants for vaccine development. Trends Immunol. 2009; 30:23–32. [PubMed: 19059004]
2. Correia-Pinto JF, Csaba N, Alonso MJ. Vaccine delivery carriers: insights and future perspectives. Int J Pharm. 2013; 440:27–38. [PubMed: 22561794]
3. Joshi MD, Unger WJ, Storm G, van Kooyk Y, Mastrobattista E. Targeting tumor antigens to dendritic cells using particulate carriers. J Control Release. 2012; 161:25–37. [PubMed: 22580109]
4. Giudice EL, Campbell JD. Needle-free vaccine delivery. Adv Drug Deliv Rev. 2006; 20:68–89. [PubMed: 16564111]
5. Swartz MA. The physiology of the lymphatic system. Adv. Drug Deliv. Res. 2001; 50
6. Bachmann MF, T JJ. Vaccine delivery: a matter of size, geometry, kinetics and molecular patterns. Nat Rev Immunol. 2010; 10:787–796. [PubMed: 20948547]
7. Salerno-Gonçalves R, Sztein MB. Cell-mediated immunity and the challenges for vaccine development. Trends Microbiol. 2006; 14:536–542. [PubMed: 17055276]
8. Yewdell JW. Designing CD8+ T cell vaccines: it's not rocket science (yet). Curr Opin Immunol. 2010; 22:402–410. [PubMed: 20447814]
9. Amorij J-P, Kersten GFA, Saluja V, Tonnis WF, Hinrichs WLJ, Slütter B, et al. Towards tailored vaccine delivery: needs, challeges and perspectives. J Control Release. 2012; 161:363–376. [PubMed: 22245687]

10. Reddy ST, van der Vlies AJ, Simeoni E, Angeli V, Randolph GJ, O'Neil CP, et al. Exploiting lymphatic transport and complement activation in nanoparticle vaccines. Nat Biotechnol. 2007; 25:1159–1164. [PubMed: 17873867]
11. Sarikaya M, Tamerler C, Jen AK, Schulten K, Baneyx F. Molecular biomimetics: nanotechnology through biology. Nat Mater. 2003; 2:577–585. [PubMed: 12951599]
12. Sarikaya M, Tamerler C, Schwartz DT, Baneyx F. Materials assembly and formation using engineered polypeptides. Annu Rev Mater Res. 2004; 34:373–408.
13. Dickerson MB, Sandhage KH, Naik RR. Protein- and peptide directed synthesis of inorganic materials. Chem Rev. 2008; 108:4935–4978. [PubMed: 18973389]
14. Briggs BD, Knecht MR. Nanotechnology meets biology: peptide-based methods for the fabrication of functional materials. J Phys Chem Lett. 2012; 3:405–418.
15. Coyle, BL.; Zhou, W.; Baneyx, F. Protein-aided mineralization of inorganic nanostructures. In: Rehm, BHA., editor. Bionanotechnology: biological self-assembly and its applications. Norwich, U.K.: Caister Academic Press; 2013.
16. Zhou W, Schwartz DT, Baneyx F. Single pot biofabrication of zinc sulfide immunoquantum dots. J. Am. Chem. Soc. 2010; 132:4731–4738. [PubMed: 20218715]
17. Zhou W, Baneyx F. Aqueous, protein-driven synthesis of transition metal-doped ZnS immuno-quantum dots. ACS Nano. 2011; 5:8013–8018. [PubMed: 21942544]
18. Chiu D, Zhou W, Kitayaporn S, Schwartz DT, Murali-Krishna K, Kavanagh TJ, et al. Biomineralization and size control of calcium phosphate core-protein shell nanoparticles: potential for vaccine applications. Bioconjug. Chem. 2012; 23:610–617. [PubMed: 22263898]
19. Moore MW, Carbone FR, Bevan MJ. Introduction of soluble proteins into the class I pathway of antigen processing and presentation. Cell. 1988; 54:777–785. [PubMed: 3261634]
20. Kopper RA, Stallcup T, Hufford G, Liakaros CD. The 5'-end structure of ovalbumin mRNA in isolated nuclei and polysomes. Nucleic Acids Res. 1994; 22:4504–4509. [PubMed: 7971281]
21. Topham DJ, Castrucci MR, Wingo FS, Belz GT, Doherty PC. The role of antigen in the localization of naïve, acutely activated, and memory $CD8^+$ T cells to the lung during influenza pneumonia. J Immunol. 2001; 167:6983–6990. [PubMed: 11739518]
22. Urdahl KB, Liggitt D, Bevan MJ. $CD8^+$ T cells accumulate in the lungs of *Mycobacterium tuberculosis*-infected $K^{b-/-}D^{b-/-}$ mice, but provide minimal protection. J Immunol. 2003; 170:1987–1994. [PubMed: 12574368]
23. Peled JU, Kuang FL, Iglesias-Ussel MD, Roa S, Kalis SL, Goodman MF, et al. The biochemistry of somatic hypermutation. Annu Rev Immunol. 2008; 26:481–511. [PubMed: 18304001]
24. Stavnezer J, Guikema JEJ, Schrader CE. Mechanism and regulation of class switch recombination. Annu Rev Immunol. 2008; 26:261–292. [PubMed: 18370922]
25. MacLennan ICM, Gulbranson-Judge A, Toellner KM, Casamayor-Palleja M, Chan E, Sze DMY, et al. The changing preference of T and B cells for partners as T-dependent antibody responses develop. Immunol Rev. 1997; 156:53–66. [PubMed: 9176699]
26. MacLeod MKL, David A, McKee AS, Crawford F, Kappler JW, Marrack P. Memory CD4 T cells that express CXCR5 provide accelerated help to B cells. J Immunol. 2011; 186:2889–2896. [PubMed: 21270407]
27. Flynn KJ, Belz GT, Altman JD, Ahmed R, Woodland DL, Doherty PC. Virus-specific CD8+ T cells in primary and secondary influenza pneumonia. Immunity. 1998; 8:683–691. [PubMed: 9655482]
28. Reddy ST, Rehor A, Schmoekel HG, Hubbell JA, Swartz MA. In vivo targeting of dendritic cells in lymph nodes with poly(propylene sulfide) nanoparticles. J. Control. Release. 2006; 112:26–34. [PubMed: 16529839]
29. Reddy ST, Swartz MA, Hubbell JA. Targeting dendritic cells with biomaterials: developing the next generation of vaccines. Trends Immunol. 2006; 27:573–579. [PubMed: 17049307]
30. Manalova V, Flace A, Bauer M, Schwarz K, Saudan P, Bachman MF. Nanoparticles target distinct dendritic cell populations according to their size. Eur. J. Immunol. 2008; 38:1404–1413. [PubMed: 18389478]

31. Fifis T, Gamvrellis A, Crimeen-Irwin B, Pietersz GA, Li J, Mottram PL, et al. Size-dependent immunogenicity: therapeutic and protective properties of nano-vaccines against tumors. J Immunol. 2004; 173:3148–3154. [PubMed: 15322175]
32. Pfeifer JD, Wick MJ, Roberts RL, Findlay K, Normark SJ, Harding CV. Phagocytic processing of bacterial antigens for class I MHC presentation to T cells. Nature. 1993; 361:359–362. [PubMed: 7678924]
33. Harding CV, Song R. Phagocytic processing of exogenous particulate antigens by macrophages for presentation by class I MHC molecules. J Immunol. 1994; 153:4925–4933. [PubMed: 7963555]
34. Sun L, Chow LC, Frukhtbeyn SA, Bonevich JE. Preparation and properties of nanoparticles of calcium phosphate with various Ca/P ratios. J Res Natl Inst Stand Technol. 2010; 115:243–255. [PubMed: 21037948]
35. Tran KK, Shen H. The role of phagosomal pH on the size-dependent efficiency of cross-presentation by dendritic cells. Biomaterials. 2009; 30:1356–1362. [PubMed: 19091401]
36. Howland SW, Wittrup KD. Antigen release kinetics in the phagosome are critical to cross-presentation efficiency. J Immunol. 2008; 180:1576–1583. [PubMed: 18209053]
37. He Q, Mitchell AR, Johnson SL, Wagner-Bartak C, Morcol T, Bell SJD. Calcium phosphate nanoparticle adjuvant. Clin Diagn Lab Immunol. 2000; 7:899–903. [PubMed: 11063495]
38. He Q, Mitchell A, Morcol T, Bell SJD. Calcium phosphate nanoparticles induce mucosal immunity and protection against herpes simplex virus type 2. Clin Diagn Lab Immunol. 2002; 9:1021–1024. [PubMed: 12204953]
39. Tritto E, Mosca F, Gregorio E. Mechanism of action of licensed vaccine adjuvants. Vaccine. 2009; 27:3331–3334. [PubMed: 19200813]
40. Rudra JS, Tian YF, Jung JP, Collier JH. A self-assembling peptide acting as an immune adjuvant. Proc Natl Acad Sci U S A. 2010; 107:622–627. [PubMed: 20080728]
41. Ishii KJ, Akira S. Toll or toll-free adjuvant path toward the optimal vaccine development. J Clin Immunol. 2007; 27:363–371. [PubMed: 17370119]
42. Vollmer J, Krieg AM. Immunotherapeutic applications of CpG oligodeoxynucleotide TLR9 agonists. Adv Drug Deliv Rev. 2009; 28:195–204. [PubMed: 19211030]

Using rudimentary equipment and a fusion protein between a solid binding peptide and an immunogen, we achieve single-pot mineralization of ≈ 50 nm calcium phosphate core-protein shell nanoparticles. Mice vaccinated with this formulation experience robust antigen-specific $CD8^+$ T cell expansion and recall responses, highlighting the potential of immunogen-controlled adjuvant mineralization for just-in-time manufacturing of T cell vaccines.

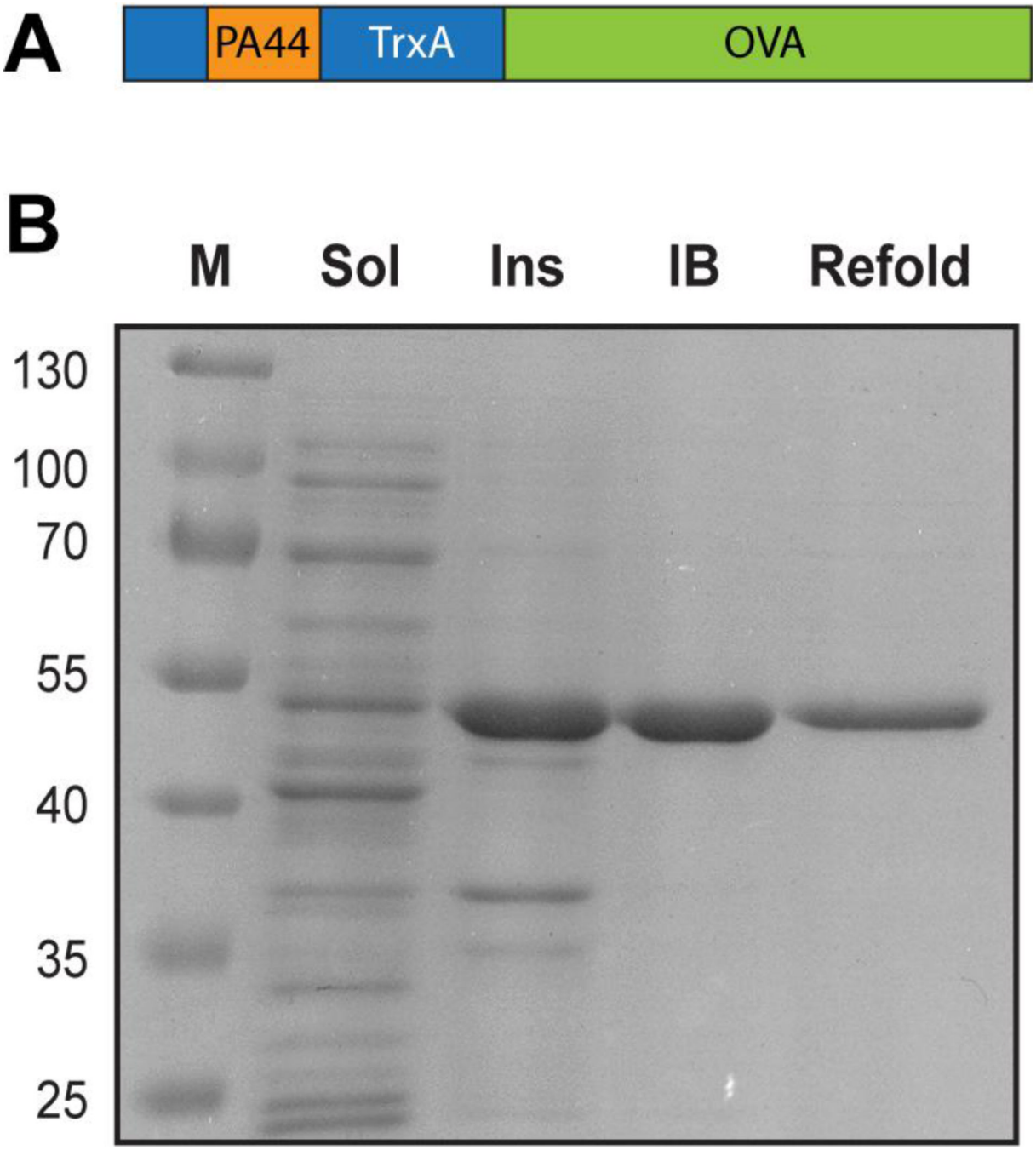

Figure 1.

(**A**) Schematic structure of the TrxA::PA44-OVA fusion protein. (**B**) SDS polyacrylamide gel analysis of soluble (Sol) and insoluble (Ins) cellular fractions and of washed inclusion bodies (IB) and refolded material (Refold). Lane M contains molecular mass markers.

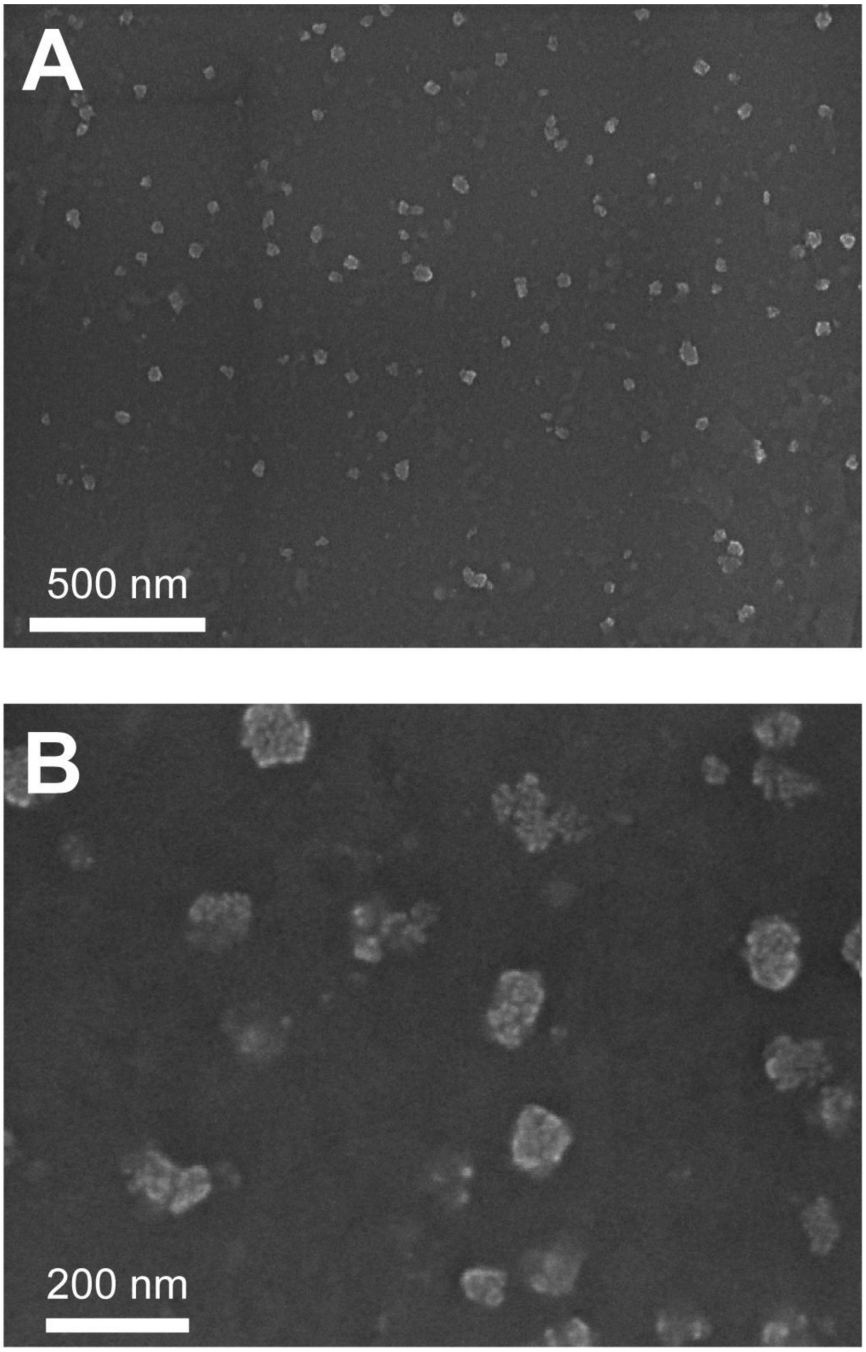

Figure 2.
SEM images of CaP nanoparticles produced in the presence of 4 μM of TrxA::PA44-Ova at low (**A**) and high (**B**) magnification.

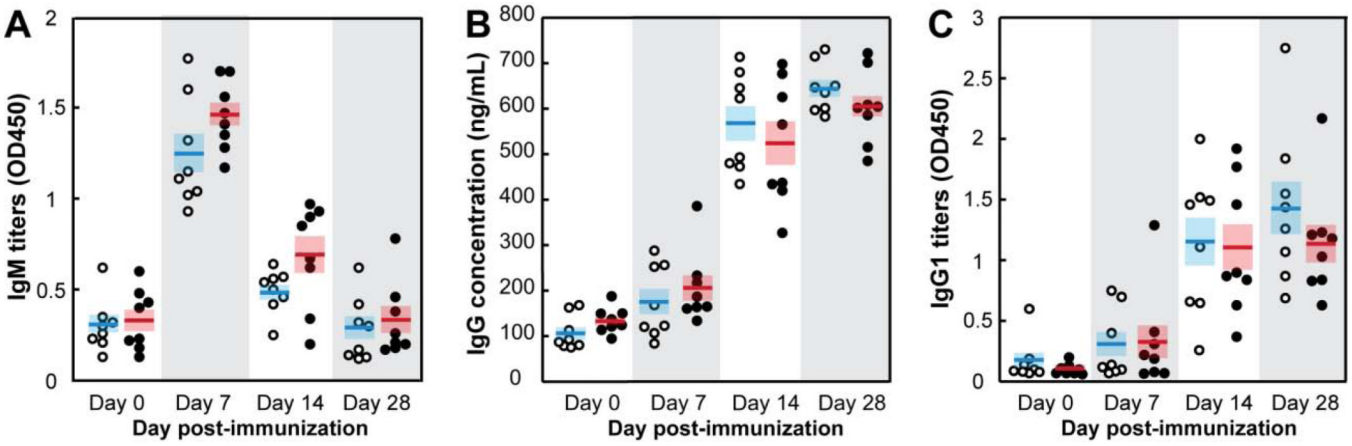

Figure 3.

Age and sex-matched wild type C57BL/6 mice (n = 8 in each group) were immunized with 18 μg of soluble TrxA::PA44-OVA protein (O) or mineralized TrxA::PA44-OVA@CaP nanoparticles (●). Mice were bled at the indicated times and the concentration of ovalbumin specific IgM (**A**), IgG (**B**) and IgG1 (**C**) antibodies was determined. Horizontal bars correspond to mean values and shaded boxes to standard errors.

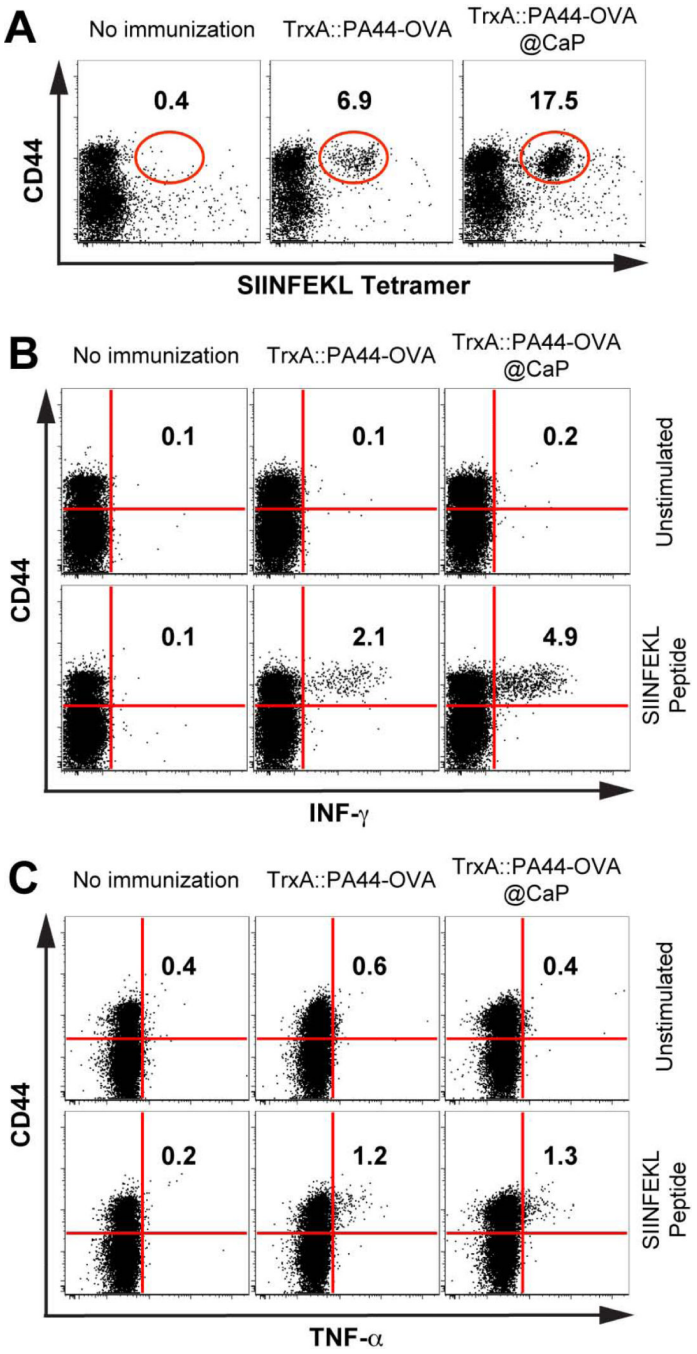

Figure 4.

Age and sex matched WT C57BL/6 were left un-immunized (n = 8) or were immunized with 18 μg of soluble TrxA::PA44-OVA (n = 8) or TrxA::PA44-OVA@CaP nanoparticles (n = 8). Four months post-immunization, one mouse per group was challenged with WSN-OVA, a recombinant influenza virus carrying ovalbumin transgene. (**A**) Lungs were excised after 12 days and single cell suspensions were analyzed for OVA-specific CD8+ T cells by flow cytometry using a monoclonal antibody against the CD44 antigen (a marker for effector-memory T cells) and $H2K^b$-restricted SIINFEKL tetramer. (**B**) Lung cells were re-

stimulated *in vitro* with the SIINFEKL peptide or left un-stimulated and IFN-γ (B) or TNF-α production (**C**) was determined using monoclonal antibodies against these cytokines.

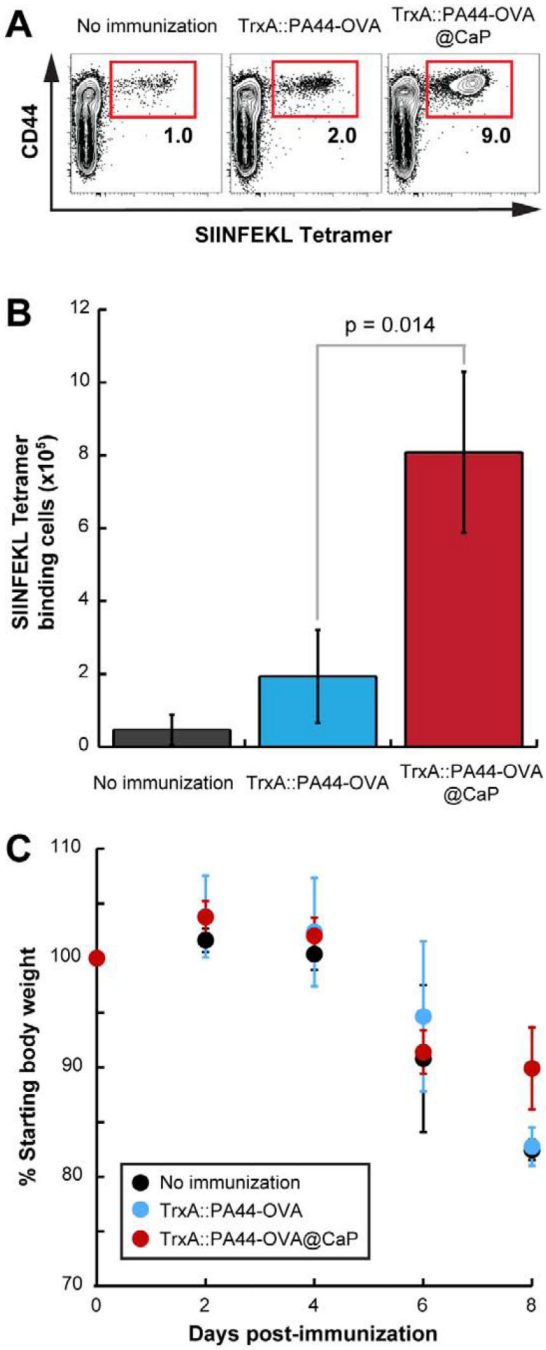

Figure 5.

Unimmunized mice (n=6) or animals from groups immunized with TrxA::PA44-OVA (n=6) or TrxA::PA44-OVA@CaP (n=6) were challenged with WSN-OVA 8 months post-vaccination. (**A**) Spleens were excised from three mice in each group after 7 days. Single cell suspensions were analyzed for OVA-specific $CD8^+$ T cells by flow cytometry using anti-CD44 antibody and $H2K^b$-restricted SIINFEKL tetramer. (**B**) Quantification of $H2K^b$-restricted SIINFEKL tetramer binding $CD8^+$ T cells from the spleen of the mice. (**C**) The remaining 3 animals in each cohort were monitored for weight loss.